

Preparation and Investigation of Composite Transparent Electrodes of Poly(3, 4-ethylenedioxythiophene) Polystyrene Sulfonate/Single-Wall Carbon Nanotubes

A. S. Voronin^{a*}, M. M. Simunin^b, F. S. Ivanchenko^c, A. V. Shiverskii^a,
Yu. V. Fadeev^c, I. A. Tambasov^d, I. V. Nemtsev^a, A. A. Matsynin^d, and S. V. Khartov^a

^a Federal Research Center “Krasnoyarsk Scientific Center,” Siberian Branch, Russian Academy of Sciences, Krasnoyarsk, 660036 Russia

^b National Research University of Electronic Technology (MIET), Moscow, 124498 Russia

^c Siberian Federal University, Krasnoyarsk, 660041 Russia

^d Kirensky Institute of Physics, Siberian Branch, Russian Academy of Sciences, Krasnoyarsk, 660036 Russia

*e-mail: a.voronin1988@mail.ru

Received January 9, 2017

Abstract—The preparation of composite transparent electrodes of poly(3, 4-ethylenedioxythiophene) polystyrene sulfonate/single-wall carbon nanotubes by the spray method is described. The influence of the successive treatment of each functional layer in acid media with different activities on the optical and electric film characteristics is considered. The composite with the surface resistance of 89 Ω/sq at the transparency of 85.3% (550 nm) on a polymer substrate is obtained.

DOI: 10.1134/S1063785017090127

Transparent electrodes based on thin films of single-wall carbon nanotubes (SWCNTs) are promising for devices of flexible and portable electronics: organic solar cells [1], LEDs [2], transparent ionistors, and capacitive and resistive sensors. However, the operating parameters of SWCNT films (110 Ω/sq at the transparency of 90% [2]) and their time-stability do not meet the requirements of the optoelectronic industry for transparent electrodes (25–50 Ω/sq at the transparency of >85%), which explains the interest of researchers in this problem.

SWCNT films are characterized by hopping conductivity, which depends on the height of the potential barriers at the sites of the contact of the nanotubes [3], whereas single nanotubes under certain conditions are characterized by ballistic transport. Thus, the SWCNT film resistance depends on the following parameters: contact resistance between the nanotubes (~0.2–2 M Ω), mean nanotube length (the length determines the contact density) [2], and nanotube conductivity [3]. The most popular method for reducing the SWCNT film resistance is doping. When the SWCNT film consists of a mixture of semiconductor and metal nanotubes, *p*-type doping is most efficient; it can be performed by treating SWCNT films with strong oxidants: HNO₃ [2], H₂SO₄, and noble-metal ions (Au³⁺ or Pt²⁺) [4]. The doping mechanism is based on the donor–acceptor interaction between the

delocalized π electrons and ions adsorbed on the lateral nanotube surface. The doping is also accompanied by partial nanotube oxidation with the grafting of the organic functional groups [3].

Another promising method for decreasing the surface resistance in SWCNT films is shunting the contact resistance between nanotubes. The shunting can be performed by polymers with the conjugated bonds (such as polyaniline [5] or poly(3, 4-ethylenedioxythiophene) polystyrene sulfonate (PEDOT : PSS) [6]. Being adsorbed on the lateral nanotube surfaces, polymer chains form new conductivity channels, which shunt the contact resistance between nanotubes [5].

The purpose of this letter is to prepare transparent electrodes with the enhanced optoelectronic characteristics and stability of the electrical properties by combining two of the most efficient approaches for increasing the conductivity of SWCNT films: *p*-type doping of nanotubes and shunting of the contact resistances by the PEDOT : PSS macromolecules.

The SWCNT films were formed by the spray method. The SWCNT aqueous dispersion (OCSiA, $C_{\text{SWCNT}} = 0.01$ wt %, sodium dodecylbenzenesulfate (SDBS) $C_{\text{SDBS}} = 0.1$ wt %) was sputtered on substrates made of polyethyleneterephthalate (50 μm) and alkaline glass (1 mm) 2.5×2.5 cm in size, heated to 130°C and subsequently dried in air (110°C, 30 min). The SWCNT film thickness was determined by the sput-

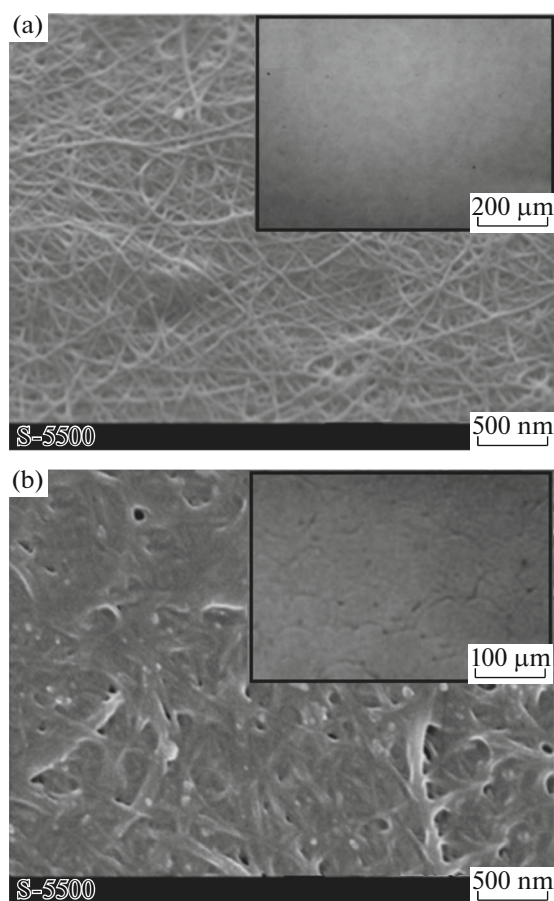


Fig. 1. SEM images of (a) SWCNT film and (b) PEDOT : PSS/SWCNT composite after CH_2O_2 exposure. The optical microscopy images are shown in the insets: (a) SWCNT film after doping and (b) PEDOT : PSS/SWCNT composite before CH_2O_2 exposure.

tered-dispersion volume: 0.015 mL/cm^2 (transparent conductive film-1 (TCF-1)), 0.03 mL/cm^2 (TCF-2), and 0.05 mL/cm^2 (TCF-3). The films were doped in HNO_3 (68%) for 60 s [2] and then washed with water and dried in air (60°C , 10 min). Silver contacts (150 nm) were deposited by magnetron sputtering.

The PEDOT : PSS aqueous solution (0.3 wt %, Sigma Aldrich) was sputtered on the SWCNT films under the conditions described above. The optimal specific volume of the sputtered dispersion was 0.1 mL/cm^2 . Afterwards, the composites were dried in air (60°C , 10 min), treated with formic acid (CH_2O_2) for 15 s [7], and subsequently dried (60°C , 10 min).

Figure 1a shows the SWCNT film images obtained by scanning electron microscopy (SEM) (Hitachi S-5500, Japan) and, after doping, optical microscopy (in the insets). The images demonstrate the high purity level and homogeneity of the SWCNT film. The doping of nanotubes is accompanied by the removal of the adsorbed SDBS molecules and organic contamina-

tions, due to which the contact resistance between the nanotubes decreases (Fig. 1a).

PEDOT : PSS sputtered on the SWCNT film demonstrates a peculiar morphology (Fig. 1b, inset) caused by the transport of the polymer phase to the periphery of a drying drop of the colloidal solution (coffee ring effect). The composite treatment in formic acid leads to the partial elution of the dielectric polymer component that solubilizes PEDOT (phosphonated polystyrene [7]) and the swelling of PEDOT : PSS, which is accompanied by the smoothing of the composite-film relief (Fig. 1b).

The spectral transmission of the composite films on the alkaline-glass substrates was measured in the range of 400–2000 nm (Shimadzu UV-3600 spectrophotometer, Japan) in all the key stages of the proposed technique. Figure 2a shows the spectral dependence of the SWCNT film (curve 1). The absorption peaks are related to the quasi-one-dimensional electronic structure of the single-wall nanotubes and caused by the van Hove singularities [3]. The peaks in this curve are assigned to semiconductor ($S_{11} \approx 1743 \text{ nm}$ and S_{22} (a weak peak; $S_{22} \approx 1116 \text{ nm}$ for thicker SWCNT films)) and metal ($M_{11} \approx 684 \text{ nm}$) nanotubes. The optoelectronic parameters of the SWCNT films are determined by the sputtered-dispersion volume. Its increase reduces the film's surface resistance and transparency (Fig. 2b): $15.64 \text{ k}\Omega/\text{sq}$ at a transparency of 95.4% at a wavelength of 550 nm (TCF-1), $4.02 \text{ k}\Omega/\text{sq}$ at 92.8% (TCF-2), and $0.81 \text{ k}\Omega/\text{sq}$ at 85.7% (TCF-3). The doping of the SWCNT films leads to an increase in the transparency in the entire range under consideration. In the range of 400–1000 nm, the transmission increases by $\sim 1.5\text{--}2\%$ and is caused by the decrease in the nanotube scattering power due to the removal of the adsorbed layers of SDBS molecules (Fig. 2a, curve 2). In the range of 1000–2000 nm, the increase in the transmission is $\sim 3\text{--}5\%$ due to the Fermi-level shift, along with the removal of the adsorbed SDBS [2]. The intensity of the absorption peak M_{11} does not change due to the insufficient shift of the Fermi level [2]. After the doping, the SWCNT films have the following parameters: $4.67 \text{ k}\Omega/\text{sq}$ at 97.1% (TCF-1), $1.44 \text{ k}\Omega/\text{sq}$ at 94.3% (TCF-2), and $277 \Omega/\text{sq}$ at 87.2% (TCF-3) (Fig. 2b).

The treatment of PEDOT : PSS with formic acid increases the transparency from 93.6 to 98.2% at a wavelength of 550 nm (Fig. 2a, curves 3, 4, respectively) and reduces the surface resistance from $10.34 \text{ M}\Omega/\text{sq}$ to $1.19 \text{ k}\Omega/\text{sq}$. The increase in the PEDOT : PSS transmission in the range of 400–1150 nm is related to the decrease in the nanotube scattering power due to the partial PSS dissolution. In the near-IR range (1150–2000 nm), on the contrary, a decrease in the film transparency is observed. A possible reason is the increase in the carrier concentration, which leads to a shift of the plasma frequency and a decrease in the of the transparency window's width.

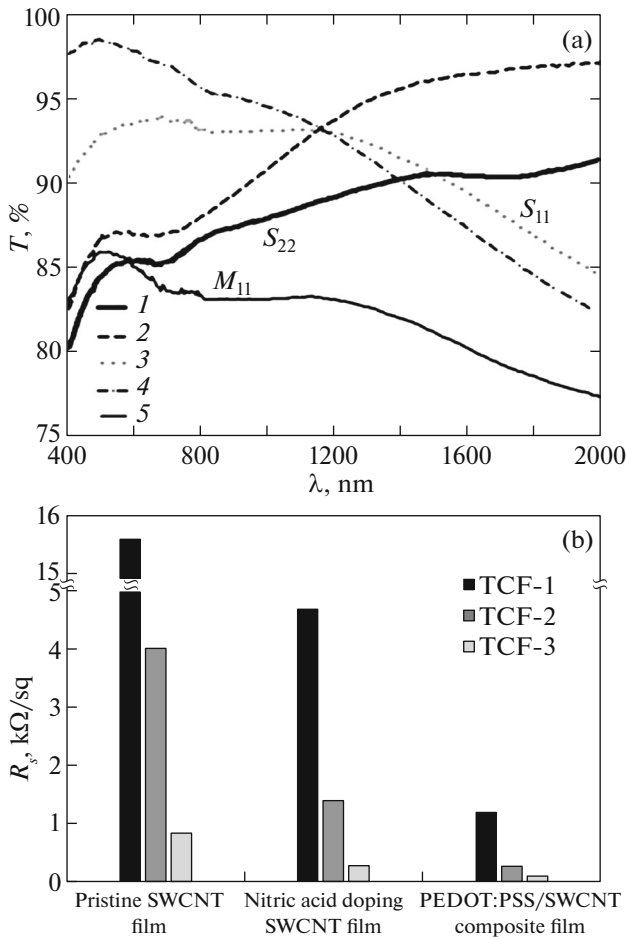


Fig. 2. (a) Spectral transparency of the PEDOT : PSS/SWCNT composite (TCF-3) on the alkaline-glass substrate in all stages of the process proposed: (1) SWCNT film, (2) SWCNT film after doping with HNO_3 , (3) PEDOT : PSS film, (4) PEDOT : PSS film treated with CH_2O_2 , and (5) PEDOT : PSS/SWCNT composite. (b) Change in the surface resistance of the PEDOT : PSS/SWCNT composites in the key preparation stages.

Thus, we observe not only the effects related to PSS removal but also the doping effect [7]. Similar changes in PEDOT : PSS films are induced by other liquids with a high permittivity level: methanol [7] and dimethyl sulfoxide.

The spectral transparency of the PEDOT : PSS/SWCNT composite films (Fig. 2a, curve 5) is due to the combination of opposing trends. In the range of 1400–2000 nm, the main contribution to the absorption is made by PEDOT : PSS (nanotubes absorb about 3–4%), and this contribution becomes smaller with a decrease in the wavelength. The tendency changes at 1158 nm, as a result of which the dominant contribution to the composite absorption in the range of 400–1100 nm is made by the carbon nanotubes. The composite films have the following characteristics: 886 Ω/sq at 95.1% (TCF-1), 283 Ω/sq

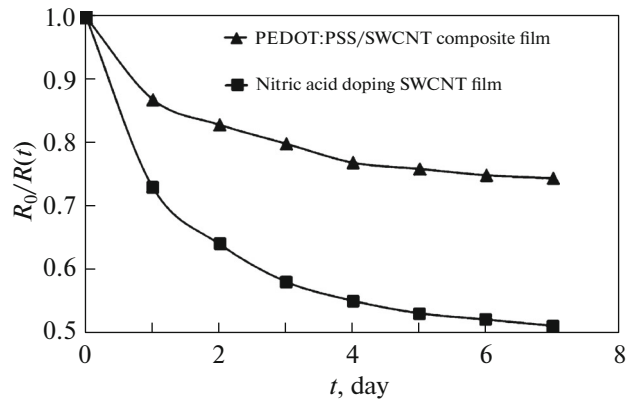


Fig. 3. Dynamics of change in the surface resistance of the doped SWCNT film and PEDOT : PSS/SWCNT composite.

at 91.9% (TCF-2), and 89 Ω/sq at 85.3% (TCF-3) (Fig. 2b). The increase in the SWCNT film thickness reduces the efficiency of this composite technique because of the low macromolecule penetrability into the porous nanotube film. The surface resistances for composites TCF-1 and TCF-3 decrease in total by factors of 17.2 and 9.2, respectively.

The key operating parameter of the transparent electrodes is the stability of the electrical parameters under normal conditions. Figure 3 shows the dynamics of the change in the absolute resistance of the composite and doped SWCNT film for a week at a temperature of $21 \pm 1^\circ\text{C}$ and humidity of $30 \pm 2\%$. For the observation time, the specific surface resistance of the composite increased by 28% and the resistance of the doped SWCNT film increased by 93%. Thus, the PEDOT : PSS layer not only shunts the contact resistances between nanotubes but also acts as a barrier layer impeding the dopant desorption, and thus increasing the system's stability.

Thus, we obtained composite transparent PEDOT : PSS/SWCNT electrodes with a surface resistance of 89 Ω/sq at a transparency of 85.3%, which is comparable to the alternative solutions. It should be noted that the stability of the electric characteristics of the composites increased by more than 65% in comparison with that for SWCNT films without polymer protection under the same conditions. The optoelectronic properties of the composites can be optimized by minimizing the amount of PEDOT : PSS due to the self-assembly of the monomolecular layer on the lateral SWCNT surface from the solution [5].

ACKNOWLEDGMENTS

This study was supported by the Russian Foundation for Basic Research (RFBR project no. 16-32-00302 mol_a) and jointly by the RFBR, Government of Krasnoyarsk Krai, and the Krasnoyarsk Krai Foundation for the Support of Scientific and Technological

Work within scientific projects nos. 16-42-243059 r_mol_a, 16-42-243006 r_mol_a, and 16-48-242092 r_ofi_m.

REFERENCES

1. M. V. Rowell, M. A. Topinka, M. D. McGehee, H.-J. Prall, G. Dennler, N. S. Sariciftci, L. Hu, and G. Grüner, *Appl. Phys. Lett.* **88**, 3506 (2006).
2. A. Kaskela, A. G. Nasibulin, M. Y. Timmermans, B. Aitchison, A. Papadimitratos, Y. Tian, Z. Zhu, H. Jiang, D. P. Brown, A. Zakhidov, and E. I. Kauppinen, *Nano Lett.* **10**, 4349 (2010).
3. D. S. Hecht, L. B. Hu, and G. Irvin, *Adv. Mater.* **23**, 1482 (2011).
4. H. C. Choi, M. Shim, S. Bangsaruntip, and H. Dai, *J. Am. Chem. Soc.* **124**, 9058 (2002).
5. A. B. Emelianov, K. F. Akhmadishina, A. V. Romashkin, V. K. Nevolin, and I. I. Bobrinetskiy, *Tech. Phys. Lett.* **41**, 94 (2015).
6. R. Jackson, B. Domercq, R. Jain, B. Kippelen, and S. Graham, *Adv. Funct. Mater.* **18**, 2548 (2008).
7. D. A. Mengistie, M. A. Ibrahim, P.-C. Wang, and C. W. Chu, *ACS Appl. Mater. Interfaces* **6**, 2292 (2014).

Translated by A. Sin'kov